PTEP

Prog. Theor. Exp. Phys. **2016**, 063B03 (13 pages)
DOI: 10.1093/ptep/ptw079

Occam's razor in lepton mass matrices: The sign of the universe's baryon asymmetry

Yuya Kaneta[1], Yusuke Shimizu[2,3], Morimitsu Tanimoto[4,*], and Tsutomu T. Yanagida[5]

[1]*Graduate School of Science and Technology, Niigata University, Niigata 950-2181, Japan*
[2]*Graduate School of Science, Hiroshima University, Higashi-Hiroshima 739-8526, Japan*
[3]*School of Physics, KIAS, Seoul 130-722, Republic of Korea*
[4]*Department of Physics, Niigata University, Niigata 950-2181, Japan*
[5]*Kavli IPMU, TODIAS, University of Tokyo, Kashiwa 277-8583, Japan*
[*]E-mail: tanimoto@muse.sc.niigata-u.ac.jp

Received April 17, 2016; Accepted May 11, 2016; Published June 30, 2016

We discuss the neutrino mass matrix based on the Occam's-razor approach in the framework of the seesaw mechanism. We impose four zeros in the Dirac neutrino mass matrix, which give the minimum number of parameters needed for the observed neutrino masses and lepton mixing angles, while the charged lepton mass matrix and the right-handed Majorana neutrino mass matrix are taken as real diagonal ones. The low-energy neutrino mass matrix has only seven physical parameters. We show successful predictions for the mixing angle θ_{13} and the CP-violating phase $\delta_{\rm CP}$ with the normal mass hierarchy of neutrinos by using the experimental data on the neutrino mass-squared differences, the mixing angles θ_{12} and θ_{23}. The most favored region of $\sin\theta_{13}$ is around 0.13–0.15, which is completely consistent with the observed value. The CP-violating phase $\delta_{\rm CP}$ is favored to be close to $\pm\pi/2$. We also discuss the Majorana phases as well as the effective neutrino mass for the neutrinoless double-beta decay m_{ee}, which is around 7–8 meV. It is extremely remarkable that we can perform a "complete experiment" to determine the low-energy neutrino mass matrix, since we have only seven physical parameters in the neutrino mass matrix. In particular, two CP-violating phases in the neutrino mass matrix are directly given by two CP-violating phases at high energy. Thus, assuming leptogenesis, we can determine the sign of the cosmic baryon in the universe from the low-energy experiments for the neutrino mass matrix.

Subject Index B40, B54

1. Introduction

The standard model has been well established by the discovery of the Higgs boson. However, the origin and structure of quark and lepton flavors are still unknown in spite of the remarkable success of the standard model. Therefore, the underlying physics of the masses and mixing of quarks and leptons is one of the fundamental problems in particle physics. A number of models have been proposed based on flavor symmetries, but there is no convincing model at present.

On the other hand, the neutrino oscillation experiments are moving onwards to reveal the CP violation in the lepton sector. The T2K experiment has confirmed the neutrino oscillation in $\nu_\mu \to \nu_e$ appearance events [1], which may provide us with new information on the CP violation in the lepton sector. Recent NOνA experimental data [2] also indicate CP violation in the neutrino oscillation. Thus, various pieces of information are now available to discuss Yukawa matrices in the lepton sector.

Funded by SCOAP[3]

Recently, the Occam's-razor approach was proposed to investigate the neutrino mass matrix [3] in the case of two heavy right-handed neutrinos. Because of tight constraints, it was shown that only the inverted mass hierarchy for the neutrinos is consistent with the present experimental data. The quark sector was also successfully discussed in this approach [4] and we found a nice prediction of the Cabibbo angle, for instance.

In this paper, we discuss the seesaw mechanism [5,6] (see also Ref. [7]) with three right-handed heavy Majorana neutrinos, predicting the normal mass hierarchy of the light neutrinos. We impose four zeros in the Dirac neutrino mass matrix, which give the minimum number of parameters needed for the observed neutrino masses and lepton mixing angles in the normal mass hierarchy of neutrinos [8,9]. Here, the charged lepton mass matrix and the right-handed Majorana neutrino mass matrix are taken to be real diagonal ones. The Dirac neutrino mass matrix is given with five complex parameters. Among them, three phases are removed by the phase redefinition of the three left-handed neutrino fields. The remaining two phases are removed by the field–phase rotation of the right-handed neutrinos. Instead, these two phases appear in the right-handed Majorana neutrino mass matrix. After integrating the heavy right-handed neutrinos, we obtain a mass matrix of the light neutrino, which contains five real parameters and two CP-violating phases.

In the present Occam's-razor approach with the four zeros of the Dirac neutrino mass matrix, we show successful predictions of the mixing angle θ_{13} and the CP-violating phase $\delta_{\rm CP}$ with the normal mass hierarchy of neutrinos. We also discuss the Majorana phases and the effective neutrino mass of the neutrinoless double-beta decay.

It is extremely remarkable that we can perform a "complete experiment" to determine the low-energy neutrino mass matrix [10], since we have only seven physical parameters in the neutrino mass matrix. In particular, two CP-violating phases in the neutrino mass matrix are directly related to two CP-violating phases at high energy. Thus, assuming leptogenesis, we can determine the sign of the cosmic baryon in the universe from only the low-energy experiments for the neutrino mass matrix [11].

In Sect. 2, we show a viable Dirac neutrino mass matrix with four zeros, where we take the real diagonal basis of the charged lepton mass matrix and the right-handed Majorana neutrino mass matrix. We also present qualitative discussions of our parameters in order to reproduce the two large mixing angles of neutrino flavors. In Sect. 3, we show the numerical results for our mass matrix. Section 4 is devoted to the summary. In the appendix, we show the parameter relations in our mass matrix.

2. Neutrino mass matrix

From the standpoint of the Occam's-razor approach [3,4], we discuss the neutrino mass matrix in the framework of the seesaw mechanism without assuming any symmetry. We take the real diagonal basis of the charged lepton mass matrix and the right-handed Majorana neutrino mass matrix as

$$M_E = \begin{pmatrix} m_e & 0 & 0 \\ 0 & m_\mu & 0 \\ 0 & 0 & m_\tau \end{pmatrix}_{LR}, \qquad M_R = \begin{pmatrix} M_1 & 0 & 0 \\ 0 & M_2 & 0 \\ 0 & 0 & M_3 \end{pmatrix}_{RR}. \tag{1}$$

We reduce the number of free parameters in the Dirac neutrino mass matrix by putting zero at several elements in the matrix. The four zeros of the Dirac neutrino mass matrix give us the minimum

number of parameters to reproduce the observed neutrino masses and lepton mixing angles. This is what we call the Occam's-razor approach.

The successful Dirac neutrino mass matrix with four zeros[1] is given as

$$m_D = \begin{pmatrix} 0 & A & 0 \\ A' & 0 & B \\ 0 & B' & C \end{pmatrix}_{LR}, \tag{2}$$

which has five complex parameters.[2] The three phases can be removed by the phase rotation of the three left-handed neutrino fields. This phase redefinition does not affect the lepton mixing matrix because the charged lepton mass matrix is diagonal and the phases are absorbed in the three right-handed charged lepton fields. In order to get the real matrix for the Dirac neutrino mass matrix, the remaining two phases are removed by the phase rotation of the two right-handed neutrino fields. Instead, the right-handed Majorana neutrino mass matrix becomes complex diagonal as follows:

$$M_R = \begin{pmatrix} M_1 e^{-i\phi_A} & 0 & 0 \\ 0 & M_2 e^{-i\phi_B} & 0 \\ 0 & 0 & M_3 \end{pmatrix}_{RR} = M_0 \begin{pmatrix} \frac{1}{k_1} e^{-i\phi_A} & 0 & 0 \\ 0 & \frac{1}{k_2} e^{-i\phi_B} & 0 \\ 0 & 0 & 1 \end{pmatrix}_{RR}, \tag{3}$$

where $M_0 \equiv M_3$, $k_1 = M_3/M_1$, and $k_2 = M_3/M_2$. We obtain the left-handed Majorana neutrino mass matrix after integrating out the heavy right-handed neutrinos,

$$m_\nu = m_D M_R^{-1} m_D^T = \frac{1}{M_0} \begin{pmatrix} A^2 k_2 e^{i\phi_B} & 0 & AB' k_2 e^{i\phi_B} \\ 0 & A'^2 k_1 e^{i\phi_A} + B^2 & BC \\ AB' k_2 e^{i\phi_B} & BC & B'^2 k_2 e^{i\phi_B} + C^2 \end{pmatrix}, \tag{4}$$

in which there are clearly ten parameters. However, this is expressed in terms of seven parameters by the rescaling of parameters. Let us replace the parameters by introducing the new parameters a, b, c, k_1', and k_2' as follows:

$$A = \sqrt{M_0 k_2'}\, a, \quad A' = \sqrt{M_0 k_1'}\, a, \quad B = \sqrt{M_0}\, b, \quad B' = \sqrt{M_0 k_2'}\, b, \quad C = \sqrt{M_0}\, c. \tag{5}$$

Then, the neutrino mass matrix is written as

$$m_\nu = \begin{pmatrix} a^2 K_2 e^{i\phi_B} & 0 & abK_2 e^{i\phi_B} \\ 0 & a^2 K_1 e^{i\phi_A} + b^2 & bc \\ abK_2 e^{i\phi_B} & bc & b^2 K_2 e^{i\phi_B} + c^2 \end{pmatrix}, \tag{6}$$

where

$$K_1 = k_1' k_1 = \left(\frac{A'B'}{AB}\right)^2 \frac{M_3}{M_1}, \qquad K_2 = k_2' k_2 = \left(\frac{B'}{B}\right)^2 \frac{M_3}{M_2}. \tag{7}$$

Finally, the neutrino mass matrix is expressed by five real parameters, a, b, c, K_1, K_2 and two phases ϕ_A, ϕ_B. Since we can input five pieces of experimental data for the neutrinos—the mass-squared

[1] Other four-zero textures may be available for lepton mixing. These will be discussed comprehensively in future work.

[2] $A' = 0$ corresponds to the case discussed in Ref. [3]. Thus, five-zero textures are not excluded.

differences $\Delta m^2_{\rm atm}$, $\Delta m^2_{\rm sol}$ and three lepton mixing angles θ_{23}, θ_{12}, and θ_{13}—there remain two free parameters. These two parameters are determined by the Dirac CP-violating phase $\delta_{\rm CP}$ and the effective neutrino mass m_{ee} for the neutrinoless double-beta decay [10].

Here we comment on the concern with the texture zero analysis of the left-handed neutrino mass matrix [12]. Actually, some two-zero textures of the left-handed neutrino mass matrix are consistent with the recent data [13]. On the other hand, our neutrino mass matrix of Eq. (6) is a one-zero texture. The two-zero textures are never realized without tuning between the parameters, as seen in Eq. (4), since we start with the seesaw mechanism of the neutrino masses, in which we take the right-handed Majorana neutrino mass matrix to be diagonal [14]. Although there are seven parameters in the neutrino mass matrix in Eq. (6), we can give clear predictions at large K_1 and K_2, which correspond to a large mass hierarchy among right-handed Majorana neutrinos.

We can obtain the eigenvectors by solving the eigenvalue equation of Eq. (6). The mass eigenvalues are expressed by a, b, c, K_1, K_2 and ϕ_A, ϕ_B, as seen in the appendix; we then get the lepton mixing matrix, the so-called Maki–Nakagawa–Sakata (MNS) matrix $U_{\rm MNS}$ [15,16]. It is expressed in terms of three mixing angles θ_{ij} $(i,j = 1,2,3;\ i < j)$, the CP-violating Dirac phase $\delta_{\rm CP}$, and two Majorana phases α and β as

$$U_{\rm MNS} \equiv \begin{pmatrix} c_{12}c_{13} & s_{12}c_{13} & s_{13}e^{-i\delta_{\rm CP}} \\ -s_{12}c_{23} - c_{12}s_{23}s_{13}e^{i\delta_{\rm CP}} & c_{12}c_{23} - s_{12}s_{23}s_{13}e^{i\delta_{\rm CP}} & s_{23}c_{13} \\ s_{12}s_{23} - c_{12}c_{23}s_{13}e^{i\delta_{\rm CP}} & -c_{12}s_{23} - s_{12}c_{23}s_{13}e^{i\delta_{\rm CP}} & c_{23}c_{13} \end{pmatrix} \begin{pmatrix} e^{-i\alpha} & 0 & 0 \\ 0 & e^{-i\beta} & 0 \\ 0 & 0 & 1 \end{pmatrix}, \tag{8}$$

where c_{ij} and s_{ij} denote $\cos\theta_{ij}$ and $\sin\theta_{ij}$, respectively.

There is a CP-violating observable, the Jarlskog invariant $J_{\rm CP}$ [17], which is derived from the following relation:

$$\begin{aligned} &i\mathcal{C} \equiv [M_\nu M_\nu^\dagger, M_E M_E^\dagger]\ , \\ &\det \mathcal{C} = -2J_{\rm CP}(m_3^2 - m_2^2)(m_2^2 - m_1^2)(m_1^2 - m_3^2)(m_\tau^2 - m_\mu^2)(m_\mu^2 - m_e^2)(m_e^2 - m_\tau^2)\ , \end{aligned} \tag{9}$$

where m_1, m_2, and m_3 are neutrino masses with real numbers. The predicted one is expressed in terms of the parameters of the mass matrix elements as

$$J_{\rm CP} \simeq \frac{1}{2} F \frac{1}{(\Delta m^2_{\rm atm})^2 \Delta m^2_{\rm sol}}\ , \tag{10}$$

where

$$\begin{aligned} F = {} & 2a^2b^4c^2K_2^2\ \{b^4K_2 \sin\phi_B + a^4K_1K_2 \sin(\phi_A - \phi_B) + \\ & a^2c^2(K_1 \sin\phi_A - K_2 \sin\phi_B) + a^2b^2K_2(K_1 \sin(\phi_A + \phi_B) - K_2 \sin 2\phi_B - \sin\phi_B)\}\ . \end{aligned} \tag{11}$$

We can extract $\sin\delta_{\rm CP}$ from $J_{\rm CP}$ by using the following relation between the mixing angles, the Dirac phase, and $J_{\rm CP}$:

$$\sin\delta_{\rm CP} = J_{\rm CP}/(s_{23}c_{23}s_{12}c_{12}s_{13}c_{13}^2)\ . \tag{12}$$

The Majorana phases α and β are obtained after diagonalizing the neutrino mass matrix of Eq. (6) as follows:

$$U_{\rm MNS}^\dagger m_\nu U_{\rm MNS}^* = {\rm diag}\,\{m_1,\ m_2,\ m_3\}\ . \tag{13}$$

Then, we can estimate the effective mass that appears in the neutrinoless double-beta decay as

$$m_{ee} = c_{13}^2 c_{12}^2 e^{-2i\alpha} m_1 + c_{13}^2 s_{12}^2 e^{-2i\beta} m_2 + s_{13}^2 e^{-2i\delta_{\rm CP}} m_3 \ . \tag{14}$$

The neutrino mass matrix of Eq. (6) becomes a simple one at the K_1 and K_2 large limit with $b^2 K_2$ being finite. This case corresponds to the large hierarchy of the right-handed neutrino mass ratios M_3/M_1 and M_3/M_2. Then, the magnitudes of our parameters are estimated qualitatively to reproduce the two large mixing angles θ_{23} and θ_{12}. First, impose the maximal mixing of θ_{23}. Then, the $(2,3)$ element of Eq. (6) should be comparable to the $(3,3)$ one, so that the cancellation must be realized between two terms in the $(3,3)$ element, and then we have:

$$K_2 \sim \frac{c^2}{b^2} \ , \qquad \phi_B \sim \pm\pi \ . \tag{15}$$

The $(2,3)$ element of Eq. (6) is also comparable to the $(2,2)$ one, which is dominated by the first term $a^2 K_1 \exp(i\phi_A)$ at large K_1. So, we get

$$K_1 \sim \frac{bc}{a^2} \ . \tag{16}$$

In the next step, we impose a large θ_{12}, which requires the $(1,3)$ element of Eq. (6) to be comparable to $(2,2)$ within a few factors; therefore, we get

$$aK_1 \sim bK_2 r \ , \quad (r = 2\text{–}3) \ . \tag{17}$$

By combining Eqs. (15), (16), and (17), we obtain

$$acr \sim b^2 \ , \qquad K_1 \sim \left(\frac{c}{b}\right)^3 \ , \qquad K_2 \sim \left(\frac{c}{b}\right)^2 \ , \qquad K_1^2 \sim K_2^3 \, r^4 \ , \quad (r = 2\text{–}3) \ . \tag{18}$$

Actually, these relations are well satisfied in the numerical result at large K_1. Then, θ_{13} becomes rather large, roughly of the order of $\sin\theta_{12}/r$, since the $(1,3)$ element of Eq. (6) is comparable to $(2,3)$ within a factor of two or three. Thus, the sizable mixing angle θ_{13} is essentially derived in these textures when the observed mixing angles θ_{23} and θ_{12} are input. This situation is well reproduced in our numerical result.

Furthermore, we expect a large CP-violating phase $\delta_{\rm CP}$ in this discussion. As shown in Eq. (15), the real part of the $(3,3)$ element of Eq. (6) is significantly suppressed in order to reproduce the almost maximal mixing of θ_{23}. Then, the imaginary part of the $(3,3)$ element is relatively enhanced even if ϕ_B is close to $\pm 180^\circ$. Actually, $\phi_B \simeq \pm 175^\circ$ leads to the $\delta_{\rm CP} \simeq \pm 90^\circ$ in the numerical analysis of the next section.

3. Numerical analysis

Let us discuss the numerical result with the normal mass hierarchy of neutrinos. In the first step, we constrain the real parameters a, b, c, K_1, K_2 and two phases ϕ_A, ϕ_B by inputting the experimental data for $\Delta m^2_{\rm atm}$ and $\Delta m^2_{\rm sol}$ with 90% C.L. into the relations of Eq. (A.1) in the appendix. By removing c, ϕ_A, and ϕ_B for a fixed m_1, which is varied in the region of $m_1 = 0 \sim \sqrt{\Delta m^2_{\rm sol}}$, there remain four parameters a, b, K_1, and K_2.

In the second step, we scan them in the following regions by generating random numbers in the linear scale as follows:

$$K_1 = [1\text{–}10^6], \quad K_2 = [1\text{–}10^4], \quad a = [0\text{–}0.03]\ \mathrm{eV}^{1/2}, \quad b = [0\text{–}0.2]\ \mathrm{eV}^{1/2}. \tag{19}$$

They are constrained by the experimental data for the lepton mixing angles. We then predict δ_{CP}, m_{ee}, and the Majorana phases α and β. The input data are given as follows [18]:

$$\begin{aligned} &\Delta m^2_{\mathrm{atm}} = (2.457 \pm 0.047) \times 10^{-3}\mathrm{eV}^2\,, \qquad \Delta m^2_{\mathrm{sol}} = 7.50^{+0.19}_{-0.17} \times 10^{-5}\mathrm{eV}^2\,, \\ &\sin^2\theta_{12} = 0.304^{+0.013}_{-0.012}\,, \quad \sin^2\theta_{23} = 0.452^{+0.052}_{-0.028}\,, \quad \sin^2\theta_{13} = 0.0218 \pm 0.0010\,; \end{aligned} \tag{20}$$

we adopt these data with an error-bar of 90% C.L in our calculations. We assume the normal mass hierarchy of neutrinos. Actually, we have not found the inverted mass hierarchy, in which the three lepton mixing angles are consistent with the observed values in our numerical calculations. Thus, we consider that the normal mass hierarchy is a prediction in the present model as long as there is no extreme fine tuning of the parameters.

Let us show the result for $K_1 = 1$–5000. By inputting the data for the two mixing angles θ_{12} and θ_{23}, we present the frequency distribution of the predicted $\sin\theta_{13}$ in Fig. 1, where the vertical red lines denote the experimental data for Eq. (20) with a 3σ range. The peak is within the experimental data for the 3σ range. It is remarked that $\sin\theta_{13} \simeq 0.14$ is most favored. This prediction is understandable, as discussed below Eq. (18). We also present the frequency distribution of the predicted value of δ_{CP} in Fig. 2, where the vertical red lines denote the NOνA experimental allowed region with a 1σ range, which is obtained by the method of library event matching (LEM) [2]. We see that δ_{CP} is favored to be around ± 2 radian, which is consistent with the T2K [1] and NOνA data for the 1σ range.

If we add the constraint of the experimental data for θ_{13}, the predictions become rather clear. By inputting the experimental data for θ_{13}, we obtain the allowed region on the K_1–K_2 plane in Fig. 3. As K_1 increases, K_2 also increases gradually. This behavior is expected in Eq. (18). We present the frequency distribution of the predicted value of δ_{CP} in Fig. 4. The peak of the distribution is still around ± 2 radian, but the distribution becomes rather sharp compared with the one in Fig. 2.

Let us discuss the K_1 dependence of δ_{CP}, which is shown in Fig. 5. In the region of $K_1 = \mathcal{O}(1\text{–}100)$, the predicted δ_{CP} has a broader distribution. As K_1 increases, the predicted region gradually becomes

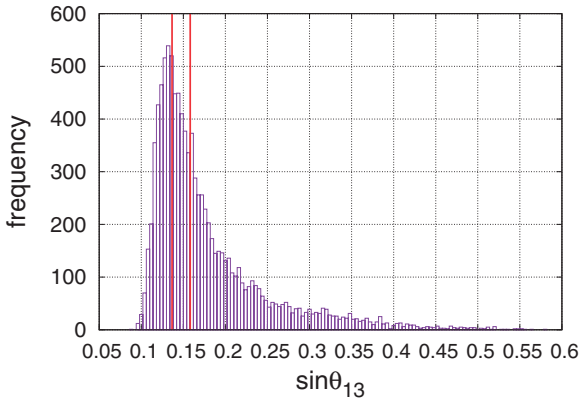

Fig. 1. The frequency distribution of the predicted $\sin\theta_{13}$ at $K_1 = 1$–5000 by inputting the data for θ_{12} and θ_{23}. Here the vertical red lines denote the experimental data with 3σ.

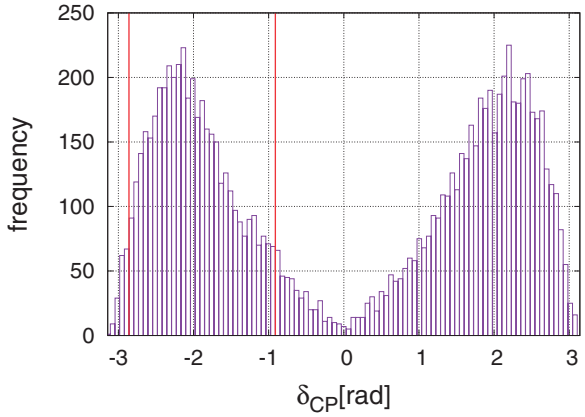

Fig. 2. The frequency distribution of the predicted $\delta_{\rm CP}$ at $K_1 = 1$–5000 by inputting the data for θ_{12} and θ_{23}. Here the vertical red lines denote the NOνA allowed region with 1σ.

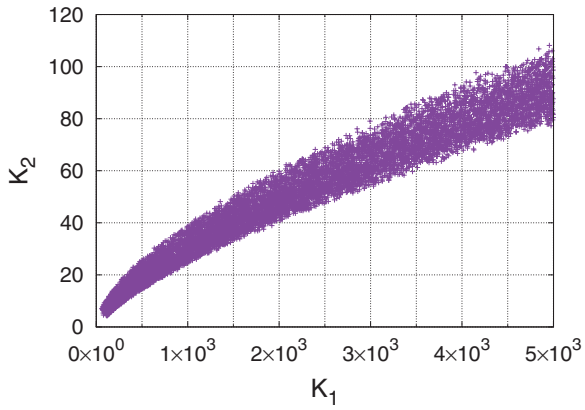

Fig. 3. The allowed region on the K_1–K_2 plane at $K_1 = 1$–5000 by inputting the data for three mixing angles.

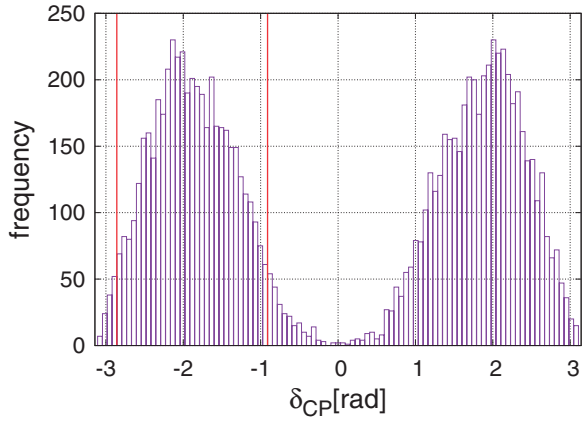

Fig. 4. The frequency distribution of the predicted $\delta_{\rm CP}$ at $K_1 = 1$–5000 by inputting the data for three mixing angles. Here the vertical red lines denote the NOνA allowed region with 1σ.

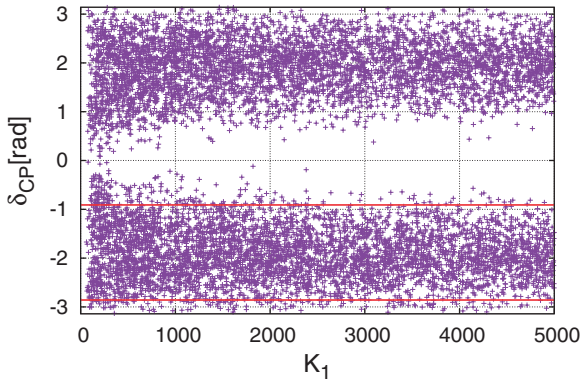

Fig. 5. The K_1 dependence of the predicted $\delta_{\rm CP}$ at $K_1 = 1$–5000 by inputting the data for three mixing angles. Here the horizontal red lines denote the NOνA experimental allowed region with 1σ.

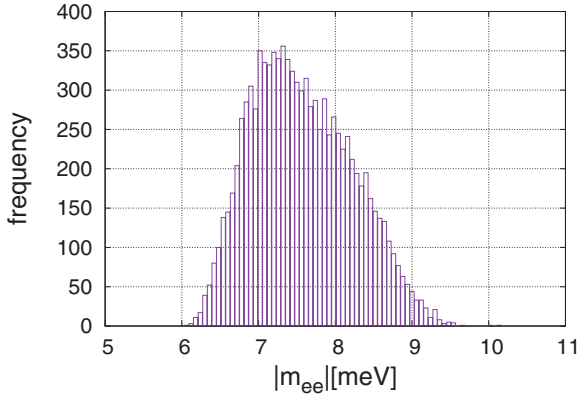

Fig. 6. The frequency distribution of the predicted m_{ee} at $K_1 = 1$–5000 by inputting the data for three mixing angles.

narrower. It then becomes consistent with the NOνA experimental allowed region with a 1σ range at high K_1.

We also predict the effective neutrino mass m_{ee}, which appears in the amplitude of the neutrinoless double-beta decay. In Fig. 6, we present the frequency distribution of m_{ee}. The favored m_{ee} is around 7 meV.

As shown in Fig. 5, our result depends on K_1. Actually, the predicted region becomes narrow as K_1 increases significantly. Let us discuss the result at $K_1 = 10^4$–10^6. We show the K_1 dependence of the predicted $\sin\theta_{13}$ at $K_1 = 10^4$–10^6 by inputting the data for θ_{12} and θ_{23} in Fig. 7. The mixing angle $\sin\theta_{13}$ is larger than 0.1 in all regions of K_1, but the large mixing angle 0.5 is allowed below $K_1 = 10^5$. However, it is remarked that $\sin\theta_{13}$ decreases gradually and converges on the experimental allowed value.

In Fig. 8, we present the frequency distribution of the predicted $\sin\theta_{13}$ by inputting the data for the two mixing angles θ_{12} and θ_{23}. The distribution becomes rather sharp compared with the case of $K_1 = 1$–5000. The most favored region of $\sin\theta_{13}$ is around 0.13–0.15, which is completely consistent with the experimental data.

In Fig. 9, we show the frequency distribution of the predicted value of $\delta_{\rm CP}$ by inputting the data for the three mixing angles. It is remarked that the peak of the frequency distributions of $\delta_{\rm CP}$ becomes

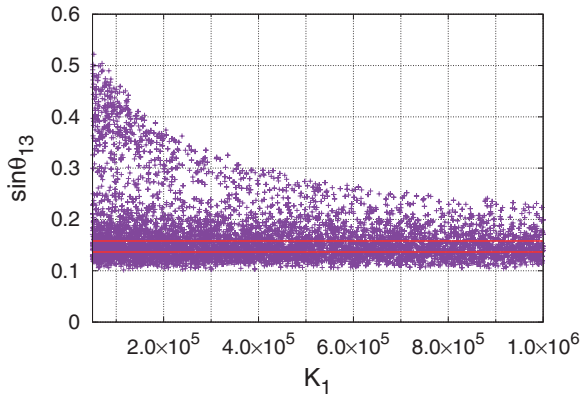

Fig. 7. The K_1 dependence of the predicted $\sin\theta_{13}$ at $K_1 = 10^4$–10^6 by inputting the data for θ_{12} and θ_{23}. Here the horizontal red lines denote the experimental data with 3σ.

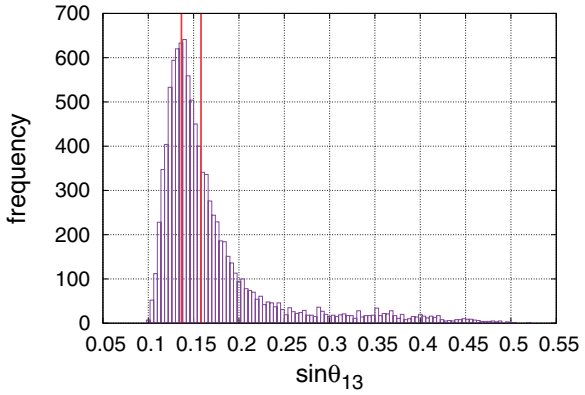

Fig. 8. The frequency distribution of the predicted $\sin\theta_{13}$ at $K_1 = 10^4$–10^6 by inputting the data for θ_{12} and θ_{23}. Here the vertical red lines denote the experimental data with 3σ.

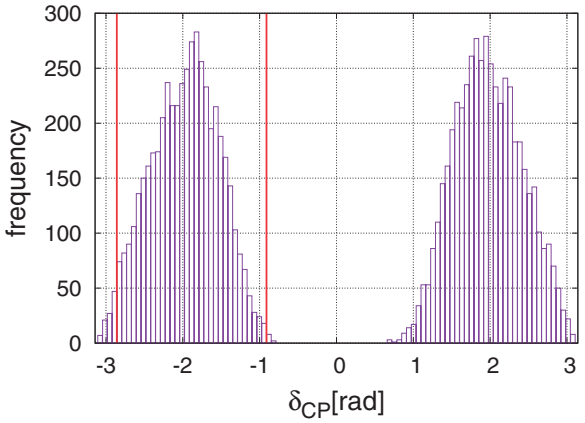

Fig. 9. The frequency distribution of the predicted $\delta_{\rm CP}$ at $K_1 = 10^4$–10^6 by inputting the data for three mixing angles. Here the vertical red lines denote the NOνA allowed region with 1σ.

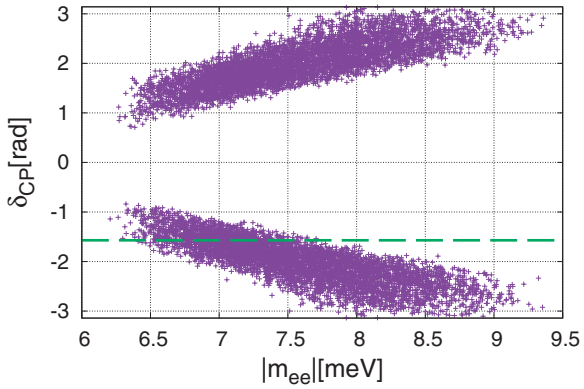

Fig. 10. The predicted Dirac phase $\delta_{\rm CP}$ versus the predicted m_{ee} at $K_1 = 10^4$–10^6 by inputting the data for three mixing angles. Here the horizontal green dashed line, inserted to guide the eye, denotes $\delta_{\rm CP} = -\pi/2$.

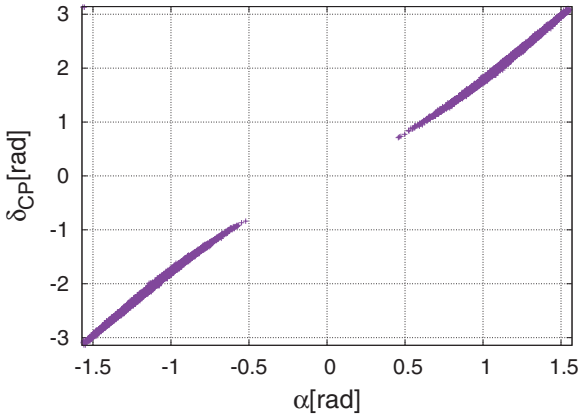

Fig. 11. The predicted Dirac phase $\delta_{\rm CP}$ versus the predicted Majorana phase α at $K_1 = 10^4$–10^6 by inputting the data for three mixing angles.

close to $\pm\pi/2$. Moreover, the region of $\delta_{\rm CP} = -1$–1 radian is almost excluded. Our result is consistent with the data for the T2K [1] and NOνA [2] experiments.

The predicted m_{ee} of the neutrinoless double-beta decay is not so changed compared with the case of $K_1 = 1$–5000. The favored value of m_{ee} is around 7–8 meV. Here, we show the predicted $\delta_{\rm CP}$ versus m_{ee} by inputting the data for three mixing angles in Fig. 10. They are rather well correlated, as seen in Eq. (A.2) in the appendix. If $\delta_{\rm CP}$ is restricted around $-\pi/2$ in the neutrino experiment, the allowed region is restricted. The predicted m_{ee} is then 6.5–8 meV.

Finally, we show the correlation between the Dirac phase $\delta_{\rm CP}$ and the Majorana phases α, β in Figs. 11, 12, and 13. There appears to be a tight correlation between them because we have only two phase parameters in the neutrino mass matrix of Eq. (6).

4. Summary

We have presented the neutrino mass matrix based on the Occam's-razor approach [3,4]. In the framework of the seesaw mechanism, we impose four zeros in the Dirac neutrino mass matrix, which give the minimum number of parameters needed for the observed neutrino masses and lepton mixing angles without assuming any flavor symmetry. Here, the charged lepton mass matrix and the right-handed Majorana neutrino mass matrix are taken to be real diagonal ones. Therefore,

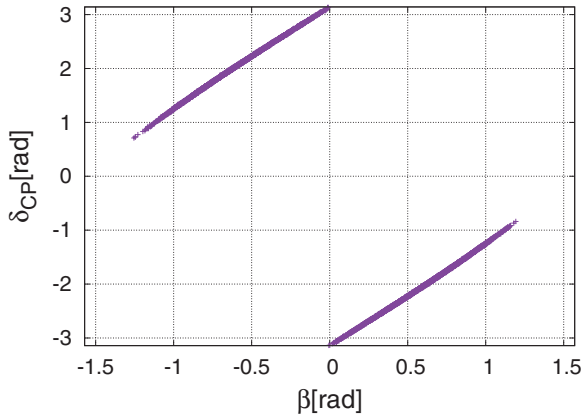

Fig. 12. The predicted Dirac phase $\delta_{\rm CP}$ versus the predicted Majorana phase β at $K_1 = 10^4$–10^6 by inputting the data for three mixing angles.

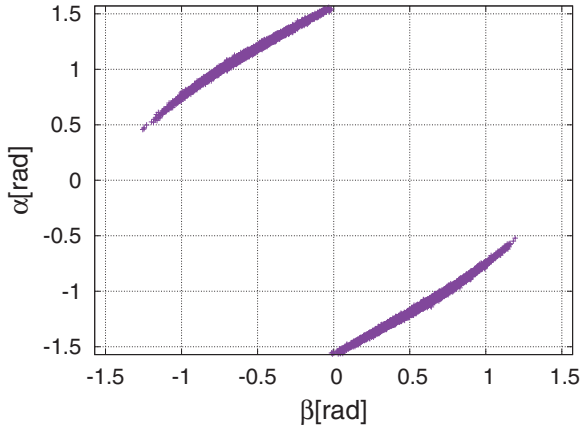

Fig. 13. The predicted Majorana phase α versus the predicted Majorana phase β at $K_1 = 10^4$–10^6 by inputting the data for three mixing angles.

the neutrino mass matrix is given with seven parameters after absorbing the three phases into the left-handed neutrino fields.

Then, we obtain the successful predictions of the mixing angle θ_{13} and the CP-violating phase $\delta_{\rm CP}$ with the normal mass hierarchy of neutrinos. We also discuss the Majorana phases α and β as well as the effective neutrino mass of the neutrinoless double-beta decay m_{ee}. In particular, as K_1 increases to 10^4–10^6, the predictions become sharper. The most favored region of $\sin\theta_{13}$ is around 0.13–0.15, which is completely consistent with the experimental data. $\delta_{\rm CP}$ is favored to be close to $\pm\pi/2$, and the effective mass m_{ee} is around 7–8 meV. The reduction of the experimental error-bar of the two mixing angles of θ_{12} and θ_{23} will provide more precise predictions in our neutrino mass matrix.

Finally, it is emphasized that we can perform a “complete experiment" to determine the low-energy neutrino mass matrix, since we have only seven physical parameters in the mass matrix (see Eq. (6)). In particular, two CP-violating phases ϕ_A and ϕ_B in the neutrino mass matrix are directly related to two CP-violating phases at high energy. Thus, assuming leptogenesis, we can determine the sign of the cosmic baryon in the universe from the low-energy experiments for the neutrino mass

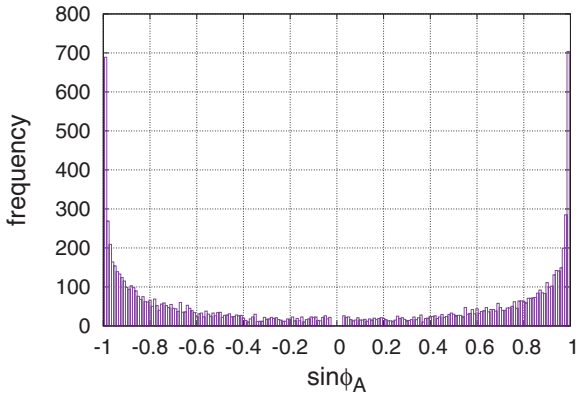

Fig. 14. The frequency distribution of the predicted $\sin\phi_A$ at $K_1 = 10^4$–10^6 by inputting the data for three mixing angles.

matrix.[3] In fact, the sign of the baryon is given by the sign of $\sin\phi_A$ for the normal mass hierarchy $M_1 < M_2 < M_3$, which is suggested from the predicted hierarchy $K_1 > K_2 > 1$ shown in Fig. 3.[4] Unfortunately, the present experimental data show both signs to be allowed, as shown in Fig. 14.[5] We expect precise measurements of the three mixing angles and CP-violating phases in low-energy experiments.

Acknowledgements

T.T.Y. thanks Prof. Serguey Petcov for the discussion on CP violation. This work is supported by JSPS Grants-in-Aid for Scientific Research (No. 28.5332; Y.S.), Scientific Research (Nos. 15K05045, 16H00862; M.T.), and Scientific Research (Nos. 26287039, 26104009, 16H02176; T.T.Y.). This work is also supported by the World Premier International Research Center Initiative (WPI Initiative), MEXT, Japan. Y.S. is supported in part by a National Research Foundation of Korea (NRF) Research Grant NRF-2015R1A2A1A05001869.

Funding

Open Access funding: SCOAP[3].

Appendix

By solving the eigenvalue equation in Eq. (6), the mass eigenvalues are expressed by a, b, c, K_1, K_2 and ϕ_A, ϕ_B. We have three equations among them as follows:

$$m_1^2 + m_2^2 + m_3^2 = c^4 + b^4(1 + K_2^2) + a^4(K_1^2 + K_2^2) + 2b^2[a^2(K_2^2 + K_1\cos\phi_A) + c^2(1 + K_2\cos\phi_B)] ,$$

$$m_1^2 m_2^2 + m_2^2 m_3^2 + m_3^2 m_1^2 = b^8 K_2^2 + a^8 K_1^2 K_2^2 + 2a^6 b^2 K_1 K_2^2 (K_1 + \cos\phi_A)$$

[3] The effect of quantum corrections of the lepton mixing matrix is neglected in the evolution from the GUT scale to the electroweak scale for the normal mass hierarchy [19].

[4] $K_{1(2)}$ is not $M_3/M_{1(2)}$ itself, as seen in Eq. (7). However, it is almost $M_3/M_{1(2)}$ as long as the Dirac neutrino mass matrix in Eq. (2) is not extremely asymmetric.

[5] A detailed discussion on this issue will be given in future work.

$$+ a^4[c^4(K_1^2 + K_2^2) + b^4K_2^2(1 + K_1^2 + 4K_1\cos\phi_A) + 2b^2c^2K_2(K_2 + K_1^2\cos\phi_B)]$$
$$+ 2a^2b^4K_2[b^2(K_2 + K_1K_2\cos\phi_A) + c^2(K_2 + K_1\cos\phi_A\cos\phi_B + K_1\sin\phi_A\sin\phi_B)] ,$$
$$m_1^2m_2^2m_3^2 = a^8c^4K_1^2K_2^2 . \tag{A.1}$$

Since the neutrino mass matrix in Eq. (6) has one zero, it constrains the observed values. Among the three mixing angles, the three phases, and the neutrino masses, there is one relation:

$$0 = c_{12}c_{13}(-s_{12}c_{23} - c_{12}s_{23}s_{13}e^{i\delta_{CP}})e^{-2i\alpha}m_1$$
$$+ s_{12}c_{13}(c_{12}c_{23} - s_{12}s_{23}s_{13}e^{i\delta_{CP}})e^{-2i\beta}m_2 + s_{13}s_{23}c_{13}e^{-i\delta_{CP}}m_3 . \tag{A.2}$$

References

[1] K. Abe et al. [T2K Collaboration], Phys. Rev. Lett. **112**, 061802 (2014) [arXiv:1311.4750 [hep-ex]] [Search INSPIRE].
[2] P. Adamson et al. [NOνA Collaboration], Phys. Rev. Lett. **116**, 151806 (2016) [arXiv:1601.05022 [hep-ex]] [Search INSPIRE].
[3] K. Harigaya, M. Ibe, and T. T. Yanagida, Phys. Rev. D **86**, 013002 (2012) [arXiv:1205.2198 [hep-ph]] [Search INSPIRE].
[4] M. Tanimoto and T. T. Yanagida, Prog. Theor. Exp. Phys. **2016**, 043B03 (2016) [arXiv:1601.04459 [hep-ph]] [Search INSPIRE].
[5] T. Yanagida, Proc. Workshop on Unified Theories and Baryon Number in the Universe, 59 (1979).
[6] M. Gell-Mann, P. Ramond, and R. Slansky, in *Supergravity*, eds. P. van Nieuwenhuizen and D. Z. Freedman (North Holland, Amsterdam, 1979).
[7] P. Minkowski, Phys. Lett. B **67**, 421 (1977).
[8] G. C. Branco, D. Emmanuel-Costa, M. N. Rebelo, and P. Roy, Phys. Rev. D **77**, 053011 (2008) [arXiv:0712.0774 [hep-ph]] [Search INSPIRE].
[9] S. Choubey, W. Rodejohann, and P. Roy, Nucl. Phys. B **808**, 272 (2009); **818**, 136 (2009) [erratum] [arXiv:0807.4289 [hep-ph]] [Search INSPIRE].
[10] G. C. Branco, R. Gonzalez Felipe, F. R. Joaquim, and T. Yanagida, Phys. Lett. B **562**, 265 (2003) [arXiv:hep-ph/0212341] [Search INSPIRE].
[11] P. H. Frampton, S. L. Glashow, and T. Yanagida, Phys. Lett. B **548**, 119 (2002) [arXiv:hep-ph/0208157] [Search INSPIRE].
[12] P. H. Frampton, S. L. Glashow, and D. Marfatia, Phys. Lett. B **536**, 79 (2002) [arXiv:hep-ph/0201008] [Search INSPIRE].
[13] M. Singh, G. Ahuja, and M. Gupta, arXiv:1603.08083 [hep-ph] [Search INSPIRE].
[14] A. Kageyama, S. Kaneko, N. Shimoyama, and M. Tanimoto, Phys. Lett. B **538**, 96 (2002) [arXiv:hep-ph/0204291] [Search INSPIRE].
[15] Z. Maki, M. Nakagawa, and S. Sakata, Prog. Theor. Phys. **28**, 870 (1962).
[16] B. Pontecorvo, Sov. Phys. JETP **26**, 984 (1968) [Zh. Eksp. Teor. Fiz. **53**, 1717 (1967)].
[17] C. Jarlskog, Phys. Rev. Lett. **55**, 1039 (1985).
[18] M. C. Gonzalez-Garcia, M. Maltoni, and T. Schwetz, Nucl. Phys. B **908**, 199 (2016) [arXiv:hep-ph/1512.06856 [hep-ph]] [Search INSPIRE].
[19] N. Haba and N. Okamura, Eur. Phys. J. C **14**, 347 (2000) [hep-ph/9906481] [Search INSPIRE].